THE JOURNAL OF PROSTHETIC DENTISTRY

CLINICAL RESEARCH

Exploring the potential of machine learning models to predict nasal measurements through facial landmarks

Remya Ampadi Ramachandran, PhD,[a] Merve Koseoglu, DDS,[b] Esra Incesu Cinka, DDS,[c] Valentim A.R. Barão, DDS, MSc, PhD,[d] Funda Bayindir, DDS, PhD,[e] Alvin G. Wee, DDS, BDS, MS, MPH, PhD,[f] Judy Chia-Chun Yuan, DDS, MS, MAS,[g] and Cortino Sukotjo, DDS, PhD, MMSc, MHPE[h]

ABSTRACT

Statement of problem. Information on predicting the measurements of the nose from selected facial landmarks to assist in maxillofacial prosthodontics is lacking.

Purpose. The objective of this study was to identify the efficiency of machine learning models in predicting the length and width of the nose from selected facial landmarks.

Material and methods. Two-dimensional frontal and lateral photographs were made of 100 men and 100 women. Different eye, nose, and ear landmarks were manually measured on the digital images. Various machine learning regression techniques were validated to confirm the accuracy of the length of the nose (LON), nasal bridge length (NBL), lateral alar width (LAW), and nasal tip protrusion (NTP).

Results. The regression models used in this study to predict the width and length of the nose parameters demonstrated a robust predictive capability, as evidenced by the high coefficient of determination score obtained (greater than 0.95). This coefficient of determination suggested the implemented model was able to effectively capture the underlying patterns and relationships within the data, leading to enhanced efficiency in predicting the outcomes. SHapley Additive ExPlanations values demonstrated that for the men-only and women-only datasets, the measurement of the auricular projection was the most important predictor of the LAW, the ear length was the most significant contributor to the LON, and the angle between the nasal bridge length and the ear length was the most significant contributor to the NBL and NTP. For the combined datasets, the distance between the superior edge of the ear to the line measuring the medial canthus width contributed most to the LON and NBL, the ear length was the most significant contributor to LAW, and the angle between the nasal bridge length and the ear length was the most significant predictor of NTP.

Conclusions. All selected algorithms provided precise width and length predictions for all data groups and were highly correlated with the actual value. The frontal images can be used to predict the LON and LAW, whereas the lateral images can be used to evaluate the NBL and NTP. (J Prosthet Dent 2025;133:1604-1613)

No conflict of interest.

[a]Graduate Faculty Associate (Fellow), 1DATA Consortium, Computational Comparative Medicine, Department of Mathematics, Kansas State University, Olathe, Olathe, Kans.
[b]Associate Professor, Department of Prosthodontics, Faculty of Dentistry, University of Sakarya, Sakarya, Turkey; and PhD student, Department of Prosthodontics, Faculty of Dentistry, University of Ataturk, Erzurum, Turkey.
[c]Asistant Professor, Department of Prosthodontics, Faculty of Dentistry, University of Sakarya, Sakarya, Turkey.
[d]Associate Professor, Department of Prosthodontics and Periodontology, Piracicaba Dental School, Universidade Estadual de Campinas (UNICAMP), Piracicaba, Sao Paulo, Brazil.
[e]Professor, Department of Prosthodontics, Faculty of Dentistry, University of Ataturk, Erzurum, Turkey.
[f]Professor, Washington Dental Service Endowed Chair in Dentistry and Chair, Department of Restorative Dentistry, University of Washington School of Dentistry, Seattle, Wash.
[g]Professor and Associate Dean for Clinical Affairs, Department of Restorative Dentistry, College of Dentistry, University of Illinois Chicago, Chicago, Ill.
[h]Professor and Chairman, Department of Prosthodontics, School of Dental Medicine, University of Pittsburgh, Pittsburgh, Pa.
[1]R.A.R. and M.K contributed equally to this article and share first authorship.

Clinical Implications

Accurate predictions of the length and width of the nose from facial landmarks indicated that the proposed model could enhance the clinical decision-making of individual men and women regarding maxillofacial prosthodontics.

Ablative tumor surgery, congenital disorders, and trauma may result in facial deformities which can impact speech, quality of life, psychological health, and social behavior.[1,2] Facial deformities have been reconstructed by using surgical procedures.[3,4] However, age, the patient's overall health, inadequate remaining tissue, vascular impairment following radiation, insufficiency of the donor locations, poor esthetics, or the patient's preferences may influence surgical reconstruction outcomes.[5,6] Prosthetic rehabilitation has been considered to be the best course of action when these constraints pose a challenge, with maxillofacial prosthetics frequently providing a lifelike rehabilitation.[1,6,7] Nose reconstruction can enhance a patient's facial appearance and treatment satisfaction, self-esteem, and social functioning, resulting in improved quality of life.[8–11]

Its unpaired nature can make the creation of a nasal prosthesis difficult.[12,13] When destruction or significant damage extends across the nose's center line and without a photograph or a cast before surgery, nose reconstruction becomes challenging.[12,13]

Developed in the 1950s, the term artificial intelligence (AI) describes the concept of creating machines that can perform jobs that are typically completed by humans. A branch of AI called machine learning (ML) uses algorithms to discover the underlying statistical structures and patterns in data, enabling the prediction of previously unobserved data.[14–17] Neural networks are popular ML models that perform better than more traditional ML algorithms, especially when dealing with complicated input structures like language or images.[14,18] Given sufficient data and computer resources, neural networks can be taught to accurately capture the underlying statistical patterns of the given data. A well-trained neural network can forecast the result of unfamiliar data by running the new data point through the network.[14]

Clinicians have used facial analysis to evaluate a patient's facial measurements, proportions, and existence of asymmetry.[19] Facial landmark detection has been evaluated in humans[20–27] using various facial landmarks, including the intermedial canthus width (MCW), the width of the face (WOF), the measure of auricular projection (MAP), the lateral alar width (LAW), the intercommissural width (ICW), the distance between the superior edge of the ear to the line measuring the medial canthus width (D1), the distance between the inferior edge of the ear to the level of the lower edge of the nose (D2), the nasal tip protrusion (NTP), the ear length (EL), the ear width (EW), and the angulation between the parallel lines of the nasal bridge length and the ear length (ANGLE), the length of the nose (LON) and the nasal bridge length (NBL).[28–35] However, none of these studies predicted the dimensions of facial features.

In dentistry, ML-based regression models have successfully predicted the width of central incisors using anthropological measurements.[36] However, the authors are unaware of studies that predicted the width and length of the nose from facial landmark measurements using ML techniques. The aim of the present study was to predict the width and length measurements of the nose from facial landmarks by using ML-based regression techniques. The research hypothesis was that ML models would exhibit high accuracy in predicting nasal parameters by using specific facial landmarks.

MATERIAL AND METHODS

The research ethics committee at Sakarya University authorized the protocol (protocol number: 71522473–050.01.04-2194531–317). Power analysis was performed by using a software program (G*Power v3.1.9.6; Heinrich-Heine-University Düsseldorf). Based on the linear regression result of a previous study,[36] the minimum sample size was 77 as a result of the regression analysis test, with 95% confidence (1-α), 95% test power (1-β), and f^2=.35 effect size. One hundred individuals per group (men and women) were selected to account for dropouts, and this study was conducted on 200 young adults aged between 18 and 24 years.

Individuals were photographed frontally and laterally in rest position with a digital single-lens reflex (DSLR) camera (Nikon D7000; Nikon Corp) equipped with a ring flash (MK-14EXT TTL; Meike) and a macro lens (90 mm Macro-Lens; Tamron) in accordance with a previously published methodology.[35,36] The camera's settings (aperture: f11, ISO:125, orientation: portrait, focus mode: auto, drive mode: single shot, image recording quality: jpeg, white balance: flash, shooting: aperture priority mode) were fixed, and a single researcher (M.K.) made the photographs; thus the standardization was maintained. The images were 300 dpi in resolution and measured 4928×3264 pixels. The Frankfurt plane was positioned parallel to the ground,[37,38] the camera lens was placed at and remained 150 cm from the participants. The camera lens was mounted on a tripod (MeFOTO Classic Aluminum; Benro) secured to the floor using a hot glue gun adhesive (S81; Somafix) to reproduce the tripod location between sessions.

A formal consent form requesting the use of their photographs in the current study was obtained from participants. The photographs had to meet certain requirements to be included in the study: eyes directed straight forward, an off-white background with no shadows on the face, and not blurred. Those who had nondeformed noses agreed to expose both ears for the photographs, had no previous facial alteration, such as plastic surgery, were above the age of 18, were able to remove their facial accessories during the study, and were willing to participate and provide consent were included in the study.

Once the photographs of 100 individuals had been collected, the minimum number of manual evaluators was also determined. As the intraclass correlation coefficient should be at least 0.75 for good inter-observer agreement,[39] it was found that 200 images should be evaluated by a minimum of 2 evaluators using 95% confidence (1-α), 95% test power (1-β), and an intraclass correlation coefficient=0.75 effect size.

Two calibrated researchers (M.K., E.I.C.) independently performed the measurements. Three independent analyses were conducted over several days to ensure the accuracy of the measures, and the outcomes were independently documented.[40] The kappa score for the agreement between the measurements performed by 2 researchers was 0.97, and the intra-observer agreement of researchers was 0.98 and 0.95, indicating a very high level of agreement.[39]

Ø1-cm red dots on the participants' foreheads were used to calibrate the dimensions of the facial metrics in each digital image. Facial landmarks, including MCW, WOF, MAP, LAW, ICW, D1, and D2 on frontal photographs and NTP, EL, EW, ANGLE, LON, and NBL on lateral photographs were measured with a photographic editing tool (ImageJ, v1.53; National Institutes of Health) (Fig. 1).[36–38,41]

Multioutput machine learning regression models were used to identify relationships between independent variables and multiple dependent numeric variables. The evaluated core models included linear regression (LR), ridge, lasso, elastic net (ELN), K-neighbors (KNN), decision tree (DT), support vector regressor (SVR), random forest (RF), and multilayer perceptron (MLP) regressors.[42] Facial landmark measurements were used as candidates for machine learning models. Facial landmarks were independent variables, and nasal landmarks were dependent or target variables.

The impact of independent variables on the final outcome was assessed by using a statistical package (Python statsmodels; Python Software Foundation) to determine the relationship between dependent variables and their predictors. The correlation coefficient matrix from the numpy Python package (Numeric Phython; Python Software Foundation) and ordinary least squares (OLS) regression from the statsmodels library (statsmodels, Python library) was used to evaluate the relationship between selected features and the target variables: LON, NBL, LAW, and NTP. The variance inflation factor (VIF) in Python confirmed the OLS regression outcomes using the statistical package (statsmodels; Python library).[43,44]

Multioutput regression can be performed through direct multioutput regression or through chained multioutput regression.[42] Mean absolute error (MAE) and coefficient-of-determination (R-squared or R^2 score) were evaluated to assess the accuracy of the regression models. The MAE metric shows the mean of the absolute difference between the predicted and actual values.[42] A lower MAE indicates that the model's

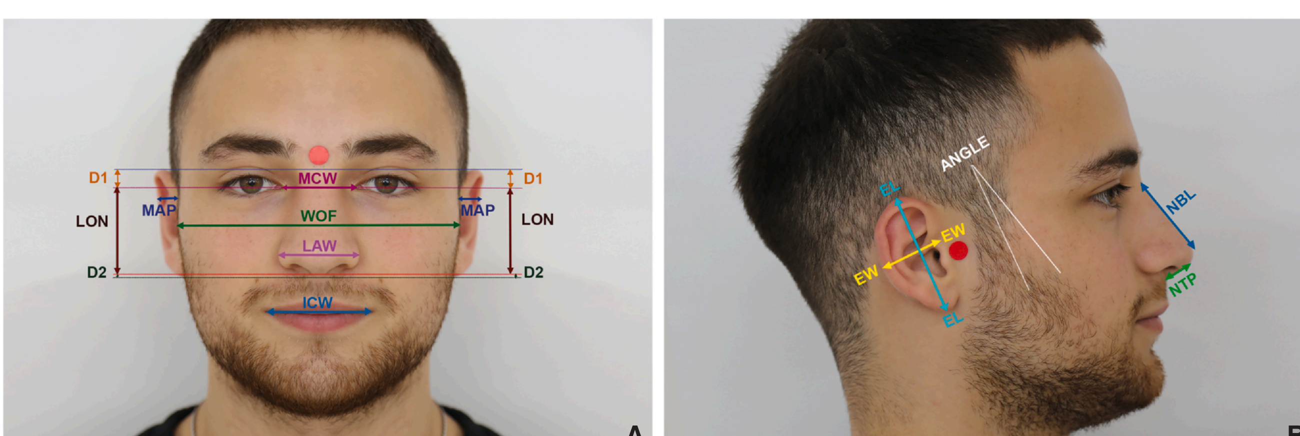

Figure 1. Visualization of facial anthropological measurements A, Intermedial canthus width (MCW), width of face (WOF), measure of auricular projection (MAP), lateral alar width (LAW), intercommissural width (ICW), distance between superior edge of ear to line measuring medial canthus width (D1), distance between inferior edge of ear to level of lower edge of nose (D2) from frontal photographs. B, Nasal tip protrusion (NTP), ear length (EL), ear width (EW), and angulation between parallel lines of nasal bridge length and ear length (ANGLE) considered in measurement and prediction of length of nose (LON) and nasal bridge length (NBL) from lateral photographs.

predictions are more accurate and closely resemble the actual data. The R^2 metric helps to determine how much of the variance in the dependent variable can be predicted by the independent variables.[40] As an initial study in esthetics predicting the length and width of the nose, these models were tested independently for their performance assessment. The advantages of multioutput regression models were leveraged, which enabled the simultaneous prediction of multiple outputs as opposed to single-target models.[42,45,46]

RESULTS

The present study analyzed 3 sets of data: men, women, and combined men and women from a young Turkish population. The data within each group revealed a significant correlation between the target variables and their predictors. When considering sex as a separate factor, a significant correlation was observed in the datasets of both the men and women (greater than 0.96). However, when the combined dataset was examined, the association was not consistent. While some variables like NTP and MAP showed a moderate association (0.48), others, such as NTP and LAW, NTP and EL, and MCW and MAP, strongly correlated (greater than 0.6). All other variables had a very strong relationship with a correlation coefficient value >0.8. The OLS results presented a high condition number, with values of 1.00e+04, 2.01e+04, and 7.90e+03, for the combined, men, and women datasets, respectively, indicating significant numbers with multicollinearity,[43] as also seen in the correlation coefficient values. The VIF analysis also confirmed the presence of high collinearity with larger design matrix values (>10) among the assessed facial anthropometric features. According to the correlation matrix (Fig. 2), there were moderate to strong correlations between the independent variables and their predictors and between the independent variables. The correlation matrix coefficients between facial anthropometric parameters ranged from 0.48 to 1.0 for the men and women combined (Fig. 2A) dataset and 0.96 to 1.0 for the men-only (Fig. 2B) and women-only dataset (Fig. 2C). The correlation coefficients also revealed a strong multicollinearity among the independent variables.

The evaluation of the feature importance score enabled predictors that significantly impacted the target prediction of the ML models to be identified. A consistent and objective explanation of these values was assessed by using the Python SHapley Additive exPlanations (SHAP) package.[17] Feature importance was also calculated by using the feature_importances_ fitted attribute of the Random Forest models.[42] The importance of features in predicting different outcomes was displayed as column plots. These plots showed the mean |SHAP| value (average impact on model output magnitude), as well as the random forest feature importance score (in the percentage of their contribution) for the combined, men-only, and women-only datasets, allowing for the comparison of feature significance across these groups for LON, NBL, LAW, and NTP (Fig. 3). The results of the scores showed that leaving out predictors such as MAP and D2 did not significantly impact the prediction of LON and NBL. Similarly, disregarding predictors such as D1, D2, and EW did not significantly impact the prediction of LAW and NTP (Fig. 3).

The ML regression models used to predict different nasal parameters such as LAW, LON, NBL, and NTP values gave an R2 score greater than 0.95, confirming the efficiency of the selected models for the given dataset. The R2 score for multioutput models with various ML models as their base are presented in Table 1, which also displays an R2 score for multioutput models greater than 0.95, indicating high accuracy for most of the models tested using a 3-fold cross-validation scheme. However, independent observations for the combined dataset revealed that the ability of LASSO and ELN models to predict NTP was relatively weak (lower than 0.92). The cross-validation scheme also helped to evaluate the problem of overfitting quantitatively. Here, the models were assessed for mean squared error (MSE) and the R2 score of the test dataset with the training dataset. The results, MSE and R2 scores, recorded for the test dataset were less than in the training dataset, indicating no chance of overfitting[42] For example, kNN showed an R2 score of 0.99, 0.98 and an MSE of 0.14, 0.11, while the RF model showed an R2 score of 0.99, 0.99 and an MSE of 0.03, 0.01 for the training and test dataset respectively. However, with the results from LASSO and ELN models, the R2 score of test data (LASSO - 0.88, ELN - 0.90) was less than the training data (LASSO - 0.89, ELN - 0.92), and the MSE of the test data (LASSO - 0.60, ELN - 0.48) was slightly greater than the training data (LASSO - 0.58, ELN - 0.47), which may be an indicator of the slight chance of overfitting with these 2 models.[42]

Figure 4 shows that the predicted results of the single output regression model closely matched the best-fit line. The RF model was used as an example to illustrate this point. The residual plot outcomes were provided for each output variable. In Figure 4, the diagonal line corresponds to the test data, while green, blue, and red circles represent predicted values for the combined, men, and women datasets, respectively. The multioutput models were successful for all 3 situations (Fig. 5A, combined men and women dataset; Fig. 5B, men-only dataset; and Fig. 5C, women-only dataset) selected for the study. In Figure 5, orange circles represent multioutput model predictions, yellow circles denote predictions from single-target models, and test data are represented by gray squares.[46]

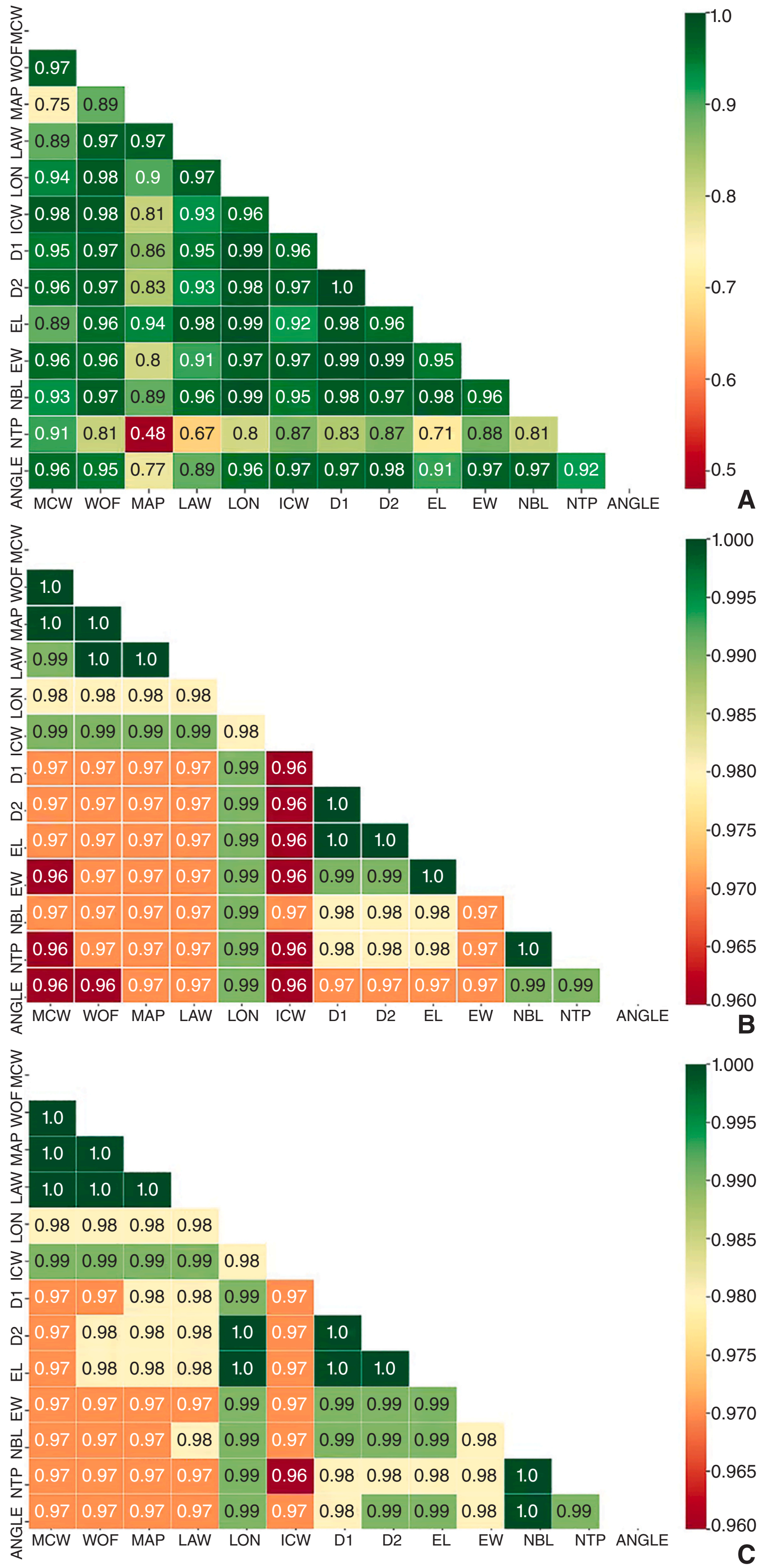

Figure 2. Correlation matrix to analyze relationship between facial anthropometric parameters for A, Men-women combined dataset. B, Men-only dataset. C, Women-only dataset.

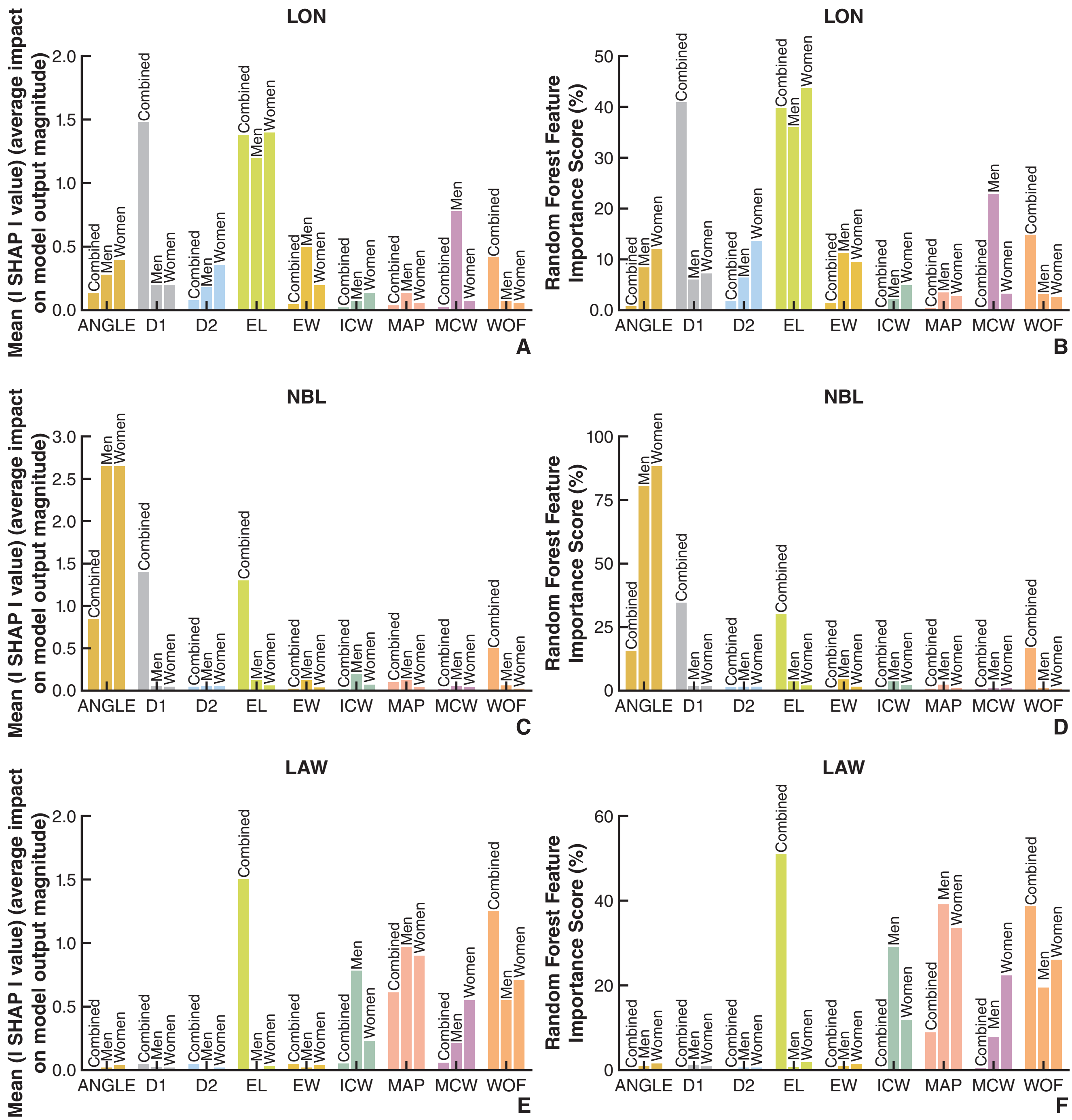

Figure 3. Representation of mean |SHAP| value (average impact on model output magnitude) and Random Forest feature importance score (%) of selected features corresponding to its contribution to ML model prediction outcome. A, B, Represents predictors of LON on combined men and women datasets, men-only dataset, and women-only dataset. C, D, Represents predictors of NBL on combined men and women datasets, men-only dataset, and women-only dataset. E. F, Represents predictors of LAW on combined men and women datasets, men-only dataset, and women-only dataset. G, H, Represents predictors of NTP on combined men and women datasets, men-only dataset, and women-only dataset.

DISCUSSION

Information on predicting the measurements of the nose from selected facial landmarks can help clinicians scientifically design maxillofacial prostheses.[36] Based on the statistical and machine learning results of the present study, a strong correlation was detected between facial landmarks and the anatomic length and width of the human nose. This study confirmed the validity of an innovative method that uses ML models in predicting

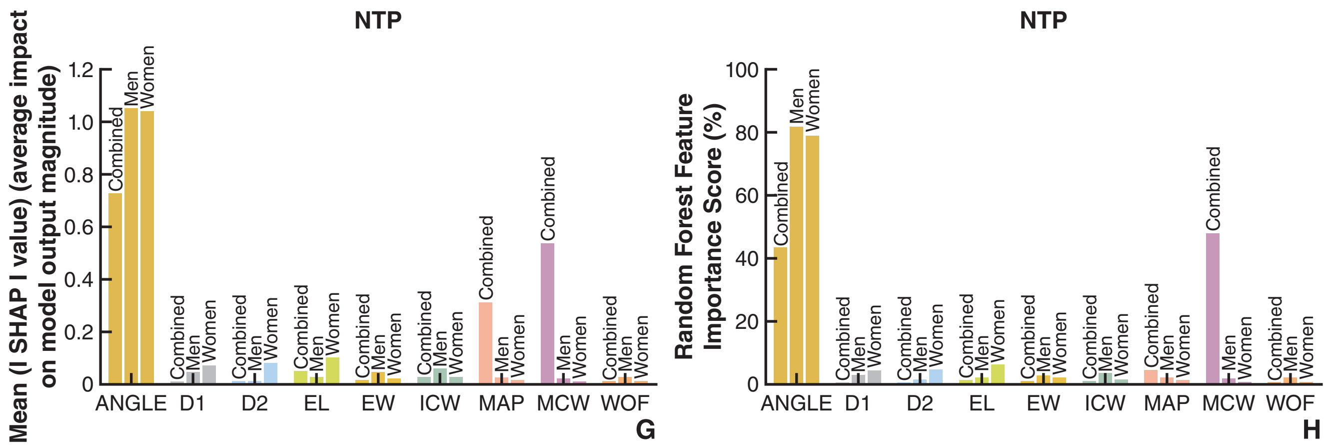

Figure 3. (*continued*)

Table 1. R2 score and ±standard deviation (SD) values of multioutput regression models for men and women only and combined datasets

Base Model	Direct Multioutput Regression			Chained Multioutput Regression		
	Combined	Men	Women	Combined	Men	Women
RandomForestRegressor	0.99 ±0.00	0.99 ±0.00	0.99 ±0.00	0.99 ±0.00	0.99 ±0.00	0.99 ±0.00
LinearSVR	0.98 ±0.01	0.97 ±0.01	0.98 ±0.01	0.98 ±0.01	0.98 ±0.01	0.98 ±0.01
DecisionTreeRegressor	0.99 ±0.00	0.99 ±0.00	0.99 ±0.00	0.99 ±0.00	0.99 ±0.00	0.99 ±0.00
KNeighborsRegressor	0.98 ±0.00	0.98 ±0.01	0.98 ±0.01	0.98 ±0.00	0.98 ±0.01	0.98 ±0.01
LinearRegression	0.99 ±0.00	0.99 ±0.00	0.99 ±0.00	0.99 ±0.00	0.99 ±0.00	0.99 ±0.00
MLPRegressor	0.97 ±0.01	0.96 ±0.02	0.96 ±0.03	0.97 ±0.02	0.96 ±0.03	0.97 ±0.01
ElasticNet	0.92 ±0.02	0.96 ±0.02	0.97 ±0.01	0.91 ±0.02	0.96 ±0.02	0.97 ±0.01
Lasso	0.89 ±0.02	0.95 ±0.02	0.96 ±0.01	0.88 ±0.02	0.95 ±0.02	0.96 ±0.01
Ridge	0.99 ±0.00	0.99 ±0.00	0.99 ±0.00	0.99 ±0.00	0.99 ±0.00	0.99 ±0.00

the length and width of the nose from the anthropologic measurements of both frontal and lateral 2-dimensional (2D).

photographs. Therefore, the research hypothesis that ML models would exhibit high accuracy for predicting nasal parameters by using specific facial landmarks was accepted.

Nasal reconstruction is a crucial aspect of facial esthetics and maxillofacial prosthetics that significantly enhances a patient's appearance, function, and quality of life.[8,9] Therefore, clinicians must develop a treatment plan that prioritizes this aspect to maximize treatment outcomes and ensure patient satisfaction. This study introduced innovative advanced technology to predict nasal features using ML techniques. The present study evaluated and highlighted the effectiveness of ML models in accurately determining these nasal features using other facial landmarks.

The authors are unaware of a previous study on using selected facial landmarks to predict the nose dimensions using ML techniques. A hybrid method that is a combination of manually recorded data and ML techniques was used in this study. Facial landmarks can be measured manually[36,37] or through automated facial landmark measurement.[38] Significant positive correlations were obtained between the facial landmark measurement results of the manual and automated methods.[38] However, the accuracy of automatic facial landmark recognition is affected by factors that include the head pose[20] and the lighting[21–23] of individuals, magnification,[24] and resolution[25–27] of images. The measurements were made by 2 independent researchers at 3 different times to test the reliability of the measurements made by the manual method. The very high intraobserver and interobserver agreement values obtained in this study established the reliability of the manual method in this study.

An obtained R2 score of over 0.95, regardless of sex, indicated high precision across most implemented models. After analyzing different models in Table 1 and considering the 0.10 MAE score achieved by the RF regression, it was concluded that the RF regressor was the optimal choice for the final model. This decision was based on the efficiency of tree-based models in predicting nasal parameters, as determined through cross-validation. Similar to other ML studies, the training and test dataset selections followed the 70:30 training:test data splitting ratio and followed an optimized hyperparameter tuning using the RandomizedSearchCV method wherever applicable. The results from the multioutput regression models are promising. Figure 5 displays 3 datasets with gray square markers for test data, orange circles for multioutput prediction, and yellow triangles for single-target prediction. In both cases, the predicted values were more accurately aligned with actual values. The 3 tested scenarios showed positive results for the multioutput models, as shown in Figure 5.

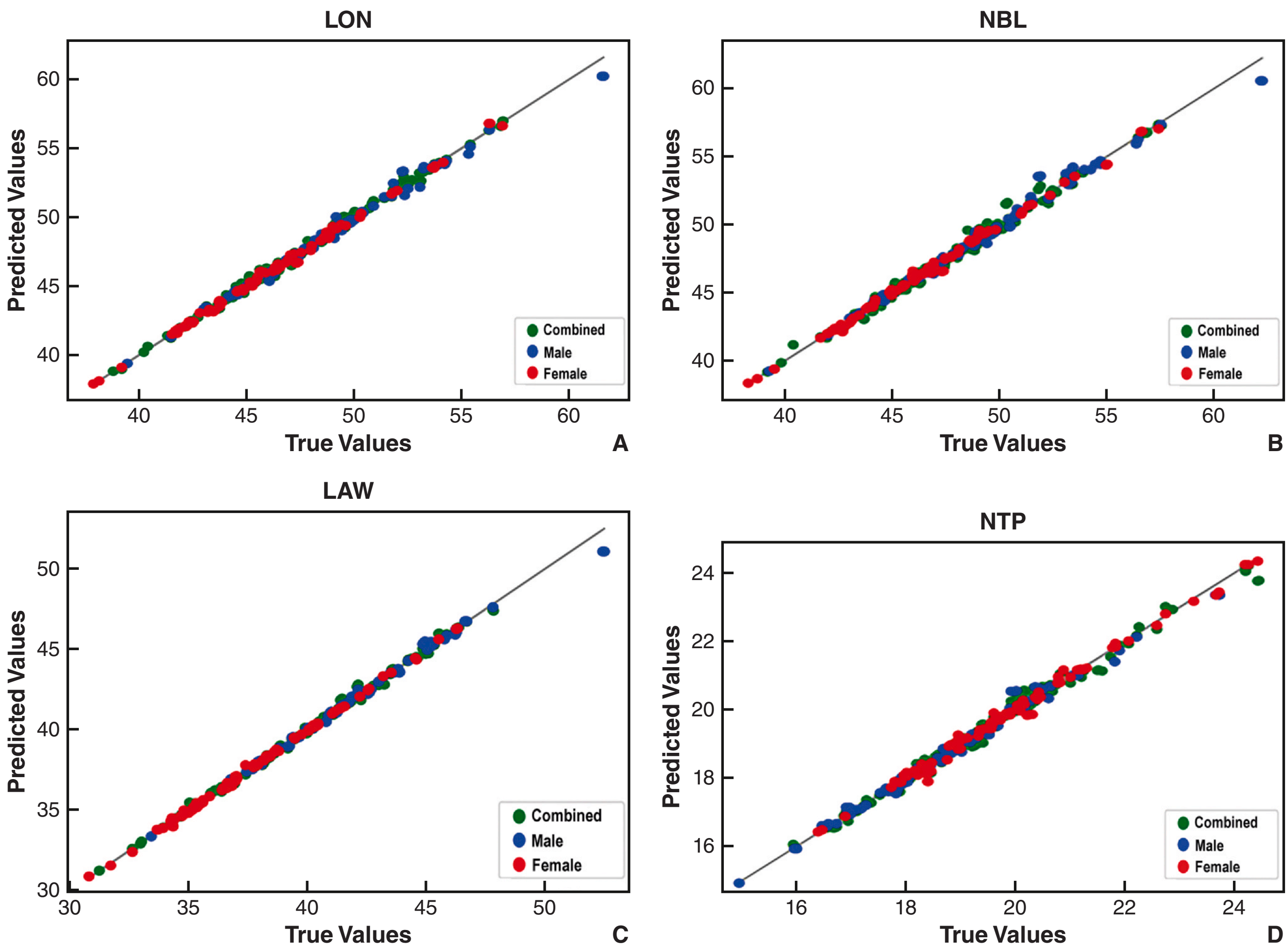

Figure 4. Predicted versus actual (true) of A, LON. B, NBL. C, LAW. D, NTP values from regression models (RF: random forest regression models). In residual plots, diagonal line (regression line), indicates best fit of test dataset, while scatters plot indicates predictions or model outcome.

The present study demonstrated that, specifically, frontal 2D images can be used to assess the LON and LAW, and lateral 2D images can be used to evaluate the NBL and NTP for men and women individually. The results of the current study were consistent with a previous study[36] in which the ML algorithm showed high performance for all situations, with an accuracy of 96%, for the prediction of central incisor tooth width using various facial landmark width in both sexes. The proposed model's ability to accurately predict nose length and width from the trials demonstrates its potential usefulness in improving clinical judgment during the fabrication of nasal prostheses.

Advancements in technology have led to the emergence of many free software programs for reconstructing images which have been extensively utilized in cosmetic surgery. The software program can create 3-dimensional (3D) models of the human face by combining 2D images from various angles, and the nose's structure can be manually adjusted to the required shape. These models enable patients to comprehensively understand the predicted nasal shape.[10] A free, open-source software program was used to generate standard tessellation language (STL) and object file format (OBJ) files that were used for rapid prototyping with 3D printers in patients who had undergone rhinoplasty.[11] In the near future, clinicians may use the proposed ML techniques to predict nose width and length parameters, enabling them to design and 3D print nasal prostheses using a similar software program.[10,11]

Limitations of the study included the participants' frontal and lateral view 2D photographs being evaluated rather than using a 3D modeling software program to enabling a more realistic analysis on different axes.[35] Moreover, although overall patterns of facial landmarks vary in different ethnicities and age groups,[28,29,31,32,34,35] this study only examined 1 one ethnicity and 1 one age group (young adults), producing a homogeneous sample[36] and resulting in a clear distinction between men and women data groups in most of the features. If the study is broadened to include different ethnic groups, it may not be feasible to overlook the unique requirements of sex-specific anthropologic features for each ethnicity while developing ML models.

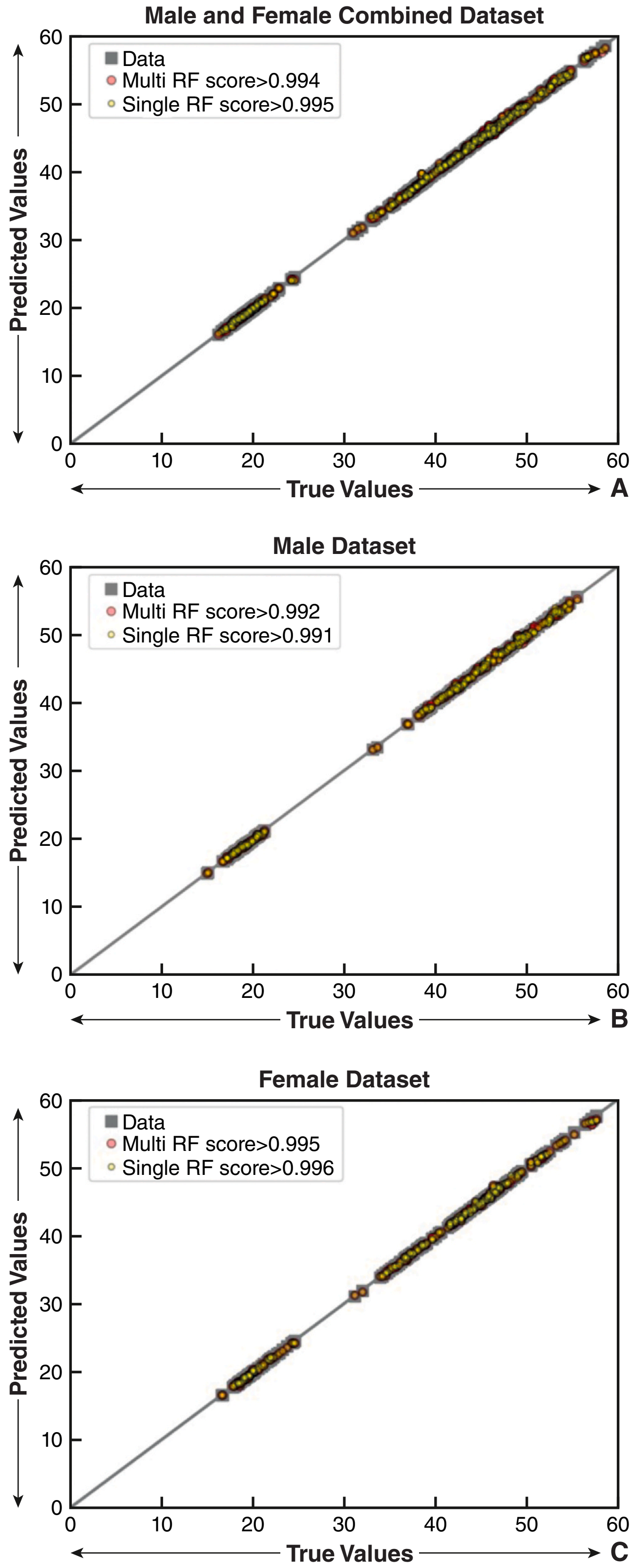

Figure 5. Comparing RF single-output and multi-output outcomes for facial anthropological parameters for same test dataset A, Men and women combined dataset. B, Men dataset only. C, Women dataset only. Test data depicted as Data, *gray squares*. Multi-output model predictions represented by *orange circles*, and prediction values from single-target models denoted by *yellow circles*.

Further studies should examine automated facial landmark detection and measurements on 3D models of different ethnicities and age groups. These studies should also explore the development of an automated web platform that can accept facial anthropological measurements and predict the length and width of the nose for potential clinical application. To further investigate this study, a strong correlation (strong multicollinearity) among the independent variables was observed. To fully comprehend the ranking or importance of these variables in predicting nasal features, additional exploration is necessary.

CONCLUSIONS

Based on the findings of this study, the following conclusions were drawn:

1. The ML regression models indicated high accuracy for predicting the width and length parameters of the nose by using specific facial landmarks (R2>.95).
2. For the men-only and women-only datasets, the measurement of auricular projection with a contribution of approximately 35% to 40% was the most important predictor of the width of the nose; the ear length with a contribution of approximately 40% was the most significant contributor to the nose length; and the angle between the nasal bridge with a contribution of approximately 80% was the most significant contributor to the nasal bridge length and nasal tip protrusion.
3. For the combined datasets, the distance between the superior edge of the ear to the medial canthus line and ear length with a contribution of approximately 35% to 40% contributed most to the length of the nose and nasal bridge length; the ear length with a contribution of around 50% was the most significant contributor to the nose width; and the angle between the nasal bridge length and intermedial canthus width with a contribution of approximately 45% to 50% was the most significant predictor of nasal tip protrusion.

PATIENT CONSENT

Participants signed a consent form that their photographs could be used in the present study.

REFERENCES

1. Scolozzi P, Jaques B. Treatment of midfacial defects using prostheses supported by ITI dental implants. *Plast Reconst Surg*. 2004;114:1395–1404.
2. Karakoca S, Aydin C, Yilmaz H, Bal BT. Retrospective study of treatment outcomes with implant-retained extraoral prostheses: Survival rates and prosthetic complications. *J Prosthet Dent*. 2010;103:118–126.
3. Cho YR, Gosain AK. Biomaterials in craniofacial reconstruction. *Clin Plast Surg*. 2004;31:377–385.
4. Antonopoulos D, Tsiliboti D, Skarpetas D, Masmanidis A. Complete orbit and forehead reconstruction using a free latissimus dorsi flap and MEDPOR implants. *Head Neck*. 2006;28:559–563.
5. Cognetti DM, Weber RS, Lai SY. Head and neck cancer: An evolving treatment paradigm. *Cancer*. 2008;113:1911–1932.
6. Hooper S, Westcott T, Evans P, Bocca A, Jagger D. Implant-supported facial prostheses provided by a maxillofacial unit in a UK regional hospital: Longevity and patient opinions. *J Prosthodont*. 2005;14:32–38.
7. Schoen PJ, Raghoebar GM, Van Oort RP, et al. Treatment outcome of bone-anchored craniofacial prostheses after tumor surgery. *Cancer*. 2001;92:3045–3050.
8. Papaspyrou G, Schick B, Schneider M, Al Kadah B. Epithetic nasal reconstruction for nasal carcinoma: Retrospective analysis on 22 patients. *Eur Arch Otorhinolaryngol*. 2017;274:867–872.
9. D'heygere V, Mattheis S, Stähr K, et al. Epithetic nasal reconstruction after total rhinectomy: Oncologic outcomes, immediate and long-term adverse effects, and quality of life. *J Plast Reconstr Aesthet Surg*. 2021;74:625–631.
10. Bekisz JM, Liss HA, Maliha SG, Witek L, Coelho PG, Flores RL. In-house manufacture of sterilizable, scaled, patient-specific 3d-printed models for rhinoplasty. *Aesthetic Surg J*. 2018;39:254–263.
11. Sobral DS, Duarte DW, Dornelles RF, Moraes CA. 3D virtual planning for rhinoplasty using a free add-on for open-source software. *Aesthetic Surg J*. 2021;41:1024–1032.
12. Reitemeier B, Götzel B, Schöne C, et al. Creation and utilization of a digital database for nasal prosthesis models. *Onkologie*. 2013;36:7–11.
13. Fantini M, De Crescenzio F, Ciocca L. Design and rapid manufacturing of anatomical prosthesis for facial rehabilitation. *Int J Interact Des Manuf*. 2013;7:51–62.
14. Schwendicke Fa, Samek W, Krois J. Artificial intelligence in dentistry: Chances and challenges. *J Dent Res*. 2020;99:769–774.
15. Shan T, Tay F, Gu L. Application of artificial intelligence in dentistry. *J Dent Res*. 2021;100:232–244.
16. Solares JRA, Raimondi FED, Zhu Y, et al. Deep learning for electronic health records: A comparative review of multiple deep neural architectures. *J Biomed Inform*. 2020;101:103337.
17. Lundberg, S. Welcome to the shap documentation- shap latest documentation. ⟨https://shap.readthedocs.io/en/latest/index.html⟩. Accessed March 11, 2024.
18. Hornik K. Approximation capabilities of multilayer feedforward networks. *Neural Netw*. 1991;4:251–257.
19. Rousseau M, Retrouvey JM. Machine learning in orthodontics: Automated facial analysis of vertical dimension for increased precision and efficiency. *Am J Orthod Dentofacial Orthop*. 2022;161:445–450.
20. Celiktutan O, Ulukaya S, Sankur B. A comparative study of face landmarking techniques. *Eurasip J Image Video Process*. 2013;2013:1–27.
21. Bodini M. A review of facial landmark extraction in 2D images and videos using deep learning. *Big Data Cogn Comput*. 2019;3:14–28.
22. Liu H, Zheng N, Wang Y, et al. Development of a face recognition system and its intelligent lighting compensation method for dark-field application. *IEEE Trans Instrum Meas*. 2021;70:1–16.
23. Fahmy G, El-Sherbeeny A, Mandala S, Abdel-Mottaleb M, Ammar H. The effect of lighting direction/condition on the performance of face recognition algorithms. *Proc SPIE Int Soc Opt Eng*. 2006;6202:188–200.
24. Li X, Liu J, Baron J, Luu K, Patterson E. Evaluating effects of focal length and viewing angle in a comparison of recent face landmark and alignment methods. *Eurasip J Image Video Process*. 2021;2021:1–18.
25. Zou WW, Yuen PC. Very low resolution face recognition problem. *IEEE Trans Image Process*. 2011;21:327–340.
26. Bartlett MS, Movellan JR, Sejnowski TJ. Face recognition by independent component analysis. *IEEE Trans Neural Netw*. 2002;13:1450–1464.
27. Nguyen K, Fookes C, Sridharan S, Tistarelli M, Nixon M. Super-resolution for biometrics: A comprehensive survey. *Pattern Recognit*. 2018;78:23–42.
28. Porter JP, Olson KL. Anthropometric facial analysis of the African American woman. *Arch Facial Plast Surg*. 2001;3:191–197.
29. Le TT, Farkas LG, Ngim RC, Levin LS, Forrest CR. Proportionality in Asian and North American Caucasian faces using neoclassical facial canons as criteria. *Aesth Plast Surg*. 2002;26:64–69.
30. Etoz BC, Etoz A, Ercan I. Nasal shapes and related differences in nostril forms: A morphometric analysis in young adults. *J Craniofac Surg*. 2008;19:1402–1408.
31. Suhk J, Park J, Nguyen AH. Nasal analysis and anatomy: Anthropometric proportional assessment in Asians-aesthetic balance from forehead to chin, part I. *Semin Plast Surg*. 2015;29:219–225.
32. Amini F, Mashayekhi Z, Rahimi H, Morad G. Craniofacial morphologic parameters in a Persian population: An anthropometric study. *J Craniofac Surg*. 2014;25:1874–1881.
33. Prasetyo AT, Putri IL. Anthropometric study of human ear: A baseline data for ear reconstruction. *J Craniofac Surg*. 2022;33:1245–1249.
34. Preeyanont P. The standard angle between the longitudinal axis of the ear and the bridge of the nose in young adult Thai women. *Showa Univ J Med Sci*. 1993;5:147–154.
35. Wang B, Dong Y, Zhao Y, Bai S, Wu G. Computed tomography measurement of the auricle in Han population of North China. *J Plast Reconstr Aesthet Surg*. 2011;64:34–40.
36. Ramachandran RA, Koseoglu M, Ozdemir H, Bayindir F, Sukotjo C. Machine learning model to predict the width of maxillary central incisor from anthropological measurements. *J Prosthodont Res*. 2024;68:432–440.
37. Ozdemir H, Koseoglu M. Relationship between different points on the face and the width of maxillary central teeth in a Turkish population. *J Prosthet Dent*. 2019;122:63–68.
38. Koseoglu M, Ramachandran RA, Ozdemir H, Ariani MD, Bayindir F, Sukotjo C. Automated facial landmark measurement using machine learning: A feasibility study. *J Prosthet Dent* 2024.
39. Koo TK, Li MY. A guideline of selecting and reporting intraclass correlation coefficients for reliability research. *J Chiropr Med*. 2016;15:155–163.
40. Li M, Cole JB, Manyama M, et al. Rapid automated landmarking for morphometric analysis of three-dimensional facial scans. *J Anat*. 2017;230:607–618.
41. Ozdemir H, Koseoglu M, Bayindir F. An investigation of the esthetic indicators of maxillary anterior teeth in young Turkish people. *J Prosthet Dent*. 2018;120:583–588.
42. Pedregosa F, Varoquaux G, Gramfort A, et al. Scikit-learn: Machine learning in Python. *J Mach Learn Res*. 2011;12:2825–2830.
43. Seabold S, Perktold J. Statsmodels: econometric and statistical modeling with python. *SciPy*. 2010;7:92–96.
44. Harris CR, Millman KJ, Van Der Walt SJ, et al. Array programming with NumPy. *Nature*. 2020;585:357–362.
45. Citing CCL- pyccl 3.0 documentation. ⟨https://ccl.readthedocs.io/en/latest/source/citation.html⟩. Accessed July 15, 2024.
46. Scikit-learn/COPYING at main·scikit-learn/scikit-learn, GitHub. Available: ⟨https://github.com/scikit-learn/scikit-learn/blob/main/COPYING⟩. Accessed July 15, 2024.

Corresponding author:
Dr Cortino Sukotjo
Department of Prosthodontics
School of Dental Medicine
University of Pittsburgh
Pittsburgh, PA 15213
Email: COS162@pitt.edu

CRediT authorship contribution statement

Remya Ampadi Ramachandran: Conceptualization, Methodology, Writing- original draft preparation, Revising and editing and Project administration. **Merve Koseoglu**: Conceptualization, Methodology, Writing- original draft preparation, Reviewing and editing, and Project administration. **Esra Incesu Cinka**: Methodology, Data collection, Data analysis, Writing. **Funda Bayindir**: Conceptualization, Methodology, Data analysis, reviewing and editing. **Valentim A. R. Barão**: Conceptualization, Methodology, Data analysis, reviewing and editing. **Alvin G. Wee**: Conceptualization, Methodology, Data analysis, reviewing and editing. **Judy Yuan**: Conceptualization, Methodology, Data analysis, reviewing and editing. **Cortino Sukotjo**: Conceptualization, Methodology, Data analysis, reviewing, supervision and editing.

https://doi.org/10.1016/j.prosdent.2024.12.012